The Company of
Biologists

RESEARCH ARTICLE

Speed-dependent modulation of wing muscle recruitment intensity and kinematics in two bat species

Nicolai Konow[1,*], Jorn A. Cheney[1], Thomas J. Roberts[1], Jose Iriarte-Díaz[2], Kenneth S. Breuer[1,3], J. Rhea S. Waldman[1,4] and Sharon M. Swartz[1,3]

ABSTRACT

Animals respond to changes in power requirements during locomotion by modulating the intensity of recruitment of their propulsive musculature, but many questions concerning how muscle recruitment varies with speed across modes of locomotion remain unanswered. We measured normalized average burst EMG (aEMG) for pectoralis major and biceps brachii at different flight speeds in two relatively distantly related bat species: the aerial insectivore *Eptesicus fuscus*, and the primarily fruit-eating *Carollia perspicillata*. These ecologically distinct species employ different flight behaviors but possess similar wing aspect ratio, wing loading and body mass. Because propulsive requirements usually correlate with body size, and aEMG likely reflects force, we hypothesized that these species would deploy similar speed-dependent aEMG modulation. Instead, we found that aEMG was speed independent in *E. fuscus* and modulated in a U-shaped or linearly increasing relationship with speed in *C. perspicillata*. This interspecific difference may be related to differences in muscle fiber type composition and/or overall patterns of recruitment of the large ensemble of muscles that participate in actuating the highly articulated bat wing. We also found interspecific differences in the speed dependence of 3D wing kinematics: *E. fuscus* modulates wing flexion during upstroke significantly more than *C. perspicillata*. Overall, we observed two different strategies to increase flight speed: *C. perspicillata* tends to modulate aEMG, and *E. fuscus* tends to modulate wing kinematics. These strategies may reflect different requirements for avoiding negative lift and overcoming drag during slow and fast flight, respectively, a subject we suggest merits further study.

KEY WORDS: Locomotor performance, Wings, Muscle activity, Lifting surface, Wing morphing, Movement economy

INTRODUCTION

Locomotion is energy demanding and most of the energy consumption is accounted for by contraction of muscles (Roberts et al., 1998; Biewener et al., 2004; Marsh et al., 2004). Conservation of energy is key in organismal ecology, and likely a substrate upon which selection acts (Weibel et al., 1998; Koteja et al., 1999). Therefore, the intensity with which limb muscles are recruited is expected to vary with locomotor demand: for example, in terrestrial locomotion,

increases in speed on the level and uphill are associated with intensified recruitment of limb extensors (Gillis and Biewener, 2001; Gillis et al., 2005; Hoyt et al., 2005; Crook et al., 2010). In fluid-based locomotion, however, the relationship between muscle recruitment intensity and the speed of flight or swimming is not expected to be linear; flapping flight, for instance, is expected to require more power at extreme than intermediate speeds due to the requirements of producing lift at low speeds and overcoming parasite and profile drag at high speeds (Pennycuick, 1968a; Rayner, 1979). Indeed, birds often modulate the intensity with which their main propulsive muscle, the pectoralis, is recruited with respect to flight speed. However, the magnitude of modulation varies in scope from negligible to substantial among species, and has been shown to be near linear for some species and U-shaped in others (Tobalske et al., 2010).

Compared with birds, we have a poor understanding of muscle function and motor control in bats (the only other extant vertebrate group capable of powered flapping flight). The fundamental pattern of activation has been measured in slow flight (<3 m s^{-1}) for several muscles in three species (*Artibeus jamaicensis*, *Antrozous pallidus* and *Eptesicus fuscus*; Hermanson and Altenbach, 1981, 1983, 1985; Foehring and Hermanson, 1984; Altenbach and Hermanson, 1987). Because of technological limitations at the time these studies were carried out, the only kinematic analysis accompanying these measurements is timing of wing tip reversal. We therefore presently lack measurements of muscle recruitment intensity across ecologically relevant flight speeds and in relation to 3D wing motions. Hence, our first aim was to determine whether pectoralis recruitment intensity changes with flight speed in two species: *Carollia perspicillata* (Linnaeus 1758) (Phyllostomidae), a frugivore that commonly flies while carrying fruit; and *Eptesicus fuscus* (Beauvois 1796) (Vespertilionidae), an insectivore that hunts insects on the wing. These species are aeroecologically distinct (Norberg and Rayner, 1987) as well as phylogenetically distantly related (Agnarsson et al., 2011); phyllostomids and vespertilionids last shared a common ancestor more than 50 million years ago (Shi and Rabosky, 2015). However, their body size (Table 1) and the span, area and aspect ratio of their wings are similar, differing no more than 5% on average in adults (Norberg and Rayner, 1987). Body anatomy and size may be expected to correlate with flight power requirements across speeds, and because speed-related changes in power demand likely are met by changes in muscle recruitment, we predicted similar speed dependence of pectoralis recruitment intensity in our two similarly built species with similar body size. Based on the lifting-line theory for fixed-wing aircraft (Pennycuick, 1968a; Rayner, 1979), as well as muscle recruitment data from birds (Tobalske et al., 2010; Askew and Ellerby, 2007; Ellerby and Askew, 2007b), we predicted that pectoralis recruitment intensity would be greater at fast and slow speeds and lowest at intermediate speeds.

Although fixed-wing aerodynamics predict a U-shaped relationship between flight speed and intensity of activity in

[1]Department of Ecology and Evolutionary Biology, Brown University, Providence, RI 02912, USA. [2]Department of Oral Biology, University of Illinois at Chicago, Chicago, IL 60612, USA. [3]School of Engineering, Brown University, Providence, RI 02912, USA. [4]Department of Ecology, Evolution, and Organismal Biology, Iowa State University, Ames, IA 50011, USA.

*Author for correspondence (Nicolai_konow@uml.edu)

N.K., 0000-0003-3310-9080

Table 1. Summary of study individual characteristics and data collected

	Carollia perspicillata				Eptesicus fuscus			
Individual	Pink	Blue	Red	Green	Green	Purple	Blue	Pink
Sex	M	F	M	M	F	M	F	M
Mass (g)	18–19	19–20	18–19	20–21	20–24	19–20	21–24	17
Experiments	4	2	2	2	4	2	3	1
Pectoralis recordings	4	2	2	2	3	1	1	1
Biceps recordings	2	2	1	2	1	1	1	1
N (EMG)	152	232	113	150	99	185	117	106
N (kinematics)	–	45	39	37	35	73	62	43

Individual refers to plot colors in Figs 2–4. N, number of wingbeats analyzed.

principal flight muscles, there are no clear predictions for muscles that function primarily to modulate wing shape. In birds, recruitment intensity of not only pectoralis, but also muscles of the shoulder and elbow are modulated with flight speed (Tobalske et al., 1997; Hedrick and Biewener, 2007; Biewener, 2011). These latter muscles include supracoracoideus, biceps brachii, humero- and scapulo-triceps, and extensor metacarpi radialis, which are important contributors to dynamic changes in wing shape (Dial et al., 1988; Robertson and Biewener, 2012). As intrinsic wing muscles control kinematics occurring distally to the shoulder as well as 3D wing geometry, and thus play major roles in modulating inertial and aerodynamic forces, they invariably influence locomotor energetics, independently of the energetic costs associated with recruitment of the primary power producers. In bats, numerous muscles of the arm and forearm, particularly the deltoideus, serratus anterior, latissimus dorsi, biceps brachii and triceps brachii, as well as intramembranous muscles of the skin of the wing membrane, may potentially contribute to controlling wing shape and orientation (Hermanson and Altenbach, 1981, 1985; Cheney et al., 2014). Here, we focused on biceps brachii, the largest intrinsic wing muscle and the main elbow flexor, asking if its recruitment is modulated with respect to flight speed.

Contraction of biceps brachii during downstroke tends to fold the wing at the elbow, prior to the beginning of upstroke. The degree of wing folding, measured as the span ratio or ratio between minimum to maximum wingspan during a wingbeat cycle, is pronounced during slow flight in fruit- and nectar-feeding bats (von Busse et al., 2012; Wolf et al., 2010), in contrast to less wing folding observed in fast flight of aerial insectivores (Hubel et al., 2016). Performing upstroke with partially folded wings tends to reduce inertial cost and negative lift (Riskin et al., 2012). The associated reduction in downward aerodynamic force may be important in slow flight, where challenges with lift production makes weight support particularly demanding (Pennycuick, 1968a; Rayner, 1979). Additionally, there may be other, as of yet, unexplored benefits from a folded wing configuration during upstroke of slow flight, which could include delayed stall and changes in net orientation of aerodynamic force. However, we focused on the possibility that wing folding likely confers aerodynamic benefits during fast flight. We hypothesized that wing folding increases at high flight speed to help reduce form drag in both species. We predicted that the aerial insectivore *E. fuscus* modulates wing folding to a greater extent than the frugivore *C. perspicillata*, consistent with an emphasis on decreasing form drag to fly fast. Finally, we predicted the recruitment intensity of biceps brachii and span ratio to be correlated across flight speeds in both species.

MATERIALS AND METHODS
Individuals used in this study (Table 1) were maintained in the Brown University Animal Care Facility, Providence, RI, USA. All housing and experimental procedures were carried out in compliance with a protocol approved by the Brown University IACUC Committee and in accordance with USDA regulations. All bats were previously trained and used regularly in wind tunnel flight studies (von Busse et al., 2013; Schunk et al., 2017). To ensure all bats were in good flight condition, they were tested in the wind tunnel at multiple speeds before recordings. All *C. perspicillata* demonstrated good flight performance in the wind tunnel. The more sedentary *E. fuscus* were able to maintain controlled steady flight in the wind tunnel after a week of training for 30 min daily.

Experiments
In order to record electromyograms (EMG), we constructed bipolar, offset hood electrodes with 1 mm pole spacing and 0.5 mm pole length (Basmajian and Stecko, 1962) from 10 cm long pieces of 0.05 mm diameter polyethylene-coated, bifilar, stainless steel wire (California Fine Wire, Grover Beach, CA, USA). An indwelling, monopolar ground electrode was made from 7 cm of stainless steel wire (Medwire, model 316SS3T, Mt Vernon, NY, USA). For each electrode, the pole ends were threaded through the bevel of a hypodermic needle, which was re-sheeted, and the other end of each electrode was soldered into a micro-connector (Digi-Key, Thief River Falls, MN, USA). Electrodes were then ethylene oxide sterilized and allowed to off-gas for five days before implantation.

Bats flew in a closed-loop, low turbulence wind tunnel at the Brown University School of Engineering, at freestream wind speeds of 0.1–7.9 m s^{-1}. The test section measured 0.60×0.82×1.5 m (height×width×length) and was delineated by mesh frames onto which the bats were able to land. Test section width was approximately four times the wingspan of the bats studied. During experiments, temperature in the wind tunnel was 22.2±1.7°C and air pressure was 101.2±0.4 kPa.

For electrode implantation, we induced anesthesia with isoflurane (1.8–3.0%) via a mask. Body temperature was maintained using a water heating pad (Gaymar, Stryker, Billerica, MA, USA) and monitored using a thermocouple. Respiratory rate was monitored visually. The skin covering the muscles of interest was gently treated for 30 s with hair removal cream (Veet, Parsippany, NJ, USA), followed by a thorough rinse with body-temperature saline. The bare skin was then sterilized with alternating scrubs of Prepodyne and chlorhexidine, and electrodes were implanted trans-cutaneously. The muscle bellies of interest, which are superficial, prominent and well delineated, were visualized under magnification through the semi-transparent skin. Care was taken to implant electrodes in the same mid-belly location across all individuals and both species for pectoralis major (posterior division), the major wing depressor, and biceps brachii (short head), the major elbow flexor. The ground electrode was implanted along the superficial sternal surface, close to the bone.

To limit tissue damage, we used the smallest possible hypodermic needle gauge, as dictated by the diameter of the

electrode wire (25 G for bifilar wire, 31 G for monopolar ground). We also took precautions to minimize artifact due to electrode motion by anchoring each electrode at the skin surface using Vetbond (3M, Chelmsford, MA, USA) and suturing the wire to the skin approximately 2 mm from the exit location using 6/0 Vicryl. All electrode wires and micro-connectors were secured to tufts of fur in several places using cyanoacrylate glue and small squares of latex sheet (2×2 cm) to avoid interference of the wing with the wire and to reduce the risk of the bat interfering physically with the implants. Each implantation procedure typically lasted approximately 20 min, after which the bat was maintained on 100% oxygen, and anatomical landmarks were highlighted for subsequent digitization using white dots (3×3 mm, at the superior margin of the sternum, shoulder, elbow, wrist and multiple joints along the digits) applied with a non-toxic paint pen (Uni-Posca PC5M, Worchester, UK). Electrodes were connected to a shielded multi-stranded cable (Cooner Wire, NMUF8/30-4046ST, Chatsworth, CA, USA), which exited the wind tunnel test section through the roof, and there joined with the impedance probes of pre-amplifiers (Grass Instruments, P511k, Warwick, RI, USA). The ground electrode interfaced via the cable shield with a serial link between the amplifier grounds, and the EMG equipment was grounded to the wind tunnel chassis.

Once awake, the bat was held in a gloved hand during recovery from anesthesia, and fed lightly when alert. Then, the bat was released into the test section, with the initial wind speed set at 3 m s⁻¹ for *C. perspicillata* and 4 m s⁻¹ for *E. fuscus*. To ensure that any deterioration of electrode quality could be detected, and to detect possible effects of anesthesia, we ran consecutive flights trials at these sequential wind speeds: 3, 4, 5, 6, 7, 1, 2, 3, 4, 5, 6, 7, 1 and 2 m s⁻¹. However, no *E. fuscus* individuals flew successfully at freestream speeds below 2 m s⁻¹.

EMG signals were amplified 1000×, with the bandpass left open (5–3000 Hz) but with a 60 Hz notch filter engaged. Signals were analog-to-digital converted (NI-DAQ 6218, National Instruments, Austin, TX, USA) and sampled at 6000 Hz using a custom script in Matlab (MathWorks, Natick, MA, USA) to the hard drive of a laptop that was battery powered during trials to minimize electromagnetic noise in the EMG.

Kinematics were recorded by three-phase-locked high-speed cameras (Photron Fastcam 1024 PCI, San Diego, CA, USA) recording at 500 Hz, and calibrated using point correspondences of a checkerboard waved through the measurement volume (Bergou et al., 2011). We used a transistor–transistor logic (TTL) signal to trigger and synchronize EMG and video. After completion of an experiment, the bat was re-anaesthetized, de-instrumented, weighed on an electronic balance (Table 1) and returned to the colony. Each bat was only used for one experiment (implantation→flight→de-instrumentation) on a given day, involving a maximum of 15 flights, and at least four days of recovery were allowed between experiments.

Measurements
Flight performance and behavior varied with speed, from steady forward flight in the test section at low freestream speeds, to almost continuous station-holding at intermediate freestream speeds, to station-holding with intermittent gliding (non-flapping) intervals, in which the bat was carried backwards in the test section, followed by resumption of flapping and return to station-holding at high freestream speeds. Given this variability, we inspected all video views of all trials to ensure that we selected wingbeats for EMG and kinematics analyses from sequences where no interference with the EMG cable occurred and where the individual was either station-holding or performing

uninterrupted forward fight without acceleration or deceleration (the latter was confirmed from 3D movements of the sternum marker). Moreover, we only analysed data from experiments where EMG was successfully collected from both muscles (see below). Table 1 provides wingbeat sample sizes for each bat.

Measurements of wingbeat kinematics
We digitized markers at the sternum, elbow, wrist and wing tip (tip of digit III) in the three video views using a custom tracker script (Bergou et al., 2011). From these landmarks, we computed 3D coordinates and used these to compute 3D angles. For the shoulder joint, we calculated the angle between the arm segment (the wing segment between the elbow and sternum marker) and the segment representing the body axis. Because we only had one body point, the sternum marker, we assumed that the body axis was parallel to the flight direction. Hence, the 3D shoulder angle was defined between the arm segment and the flight direction. Elbow angle was calculated as the 3D angle between the sternum, elbow and wrist markers with the elbow marker as vertex. Flight speed was calculated by adding the forward speed of the sternum marker to the freestream speed of the wind tunnel because animals often flew slightly faster than the ambient wind tunnel air speed. Wingbeat frequency and amplitude were calculated from the vertical position of the wrist relative to the sternum (Fig. 1). We chose not to digitize the position of the shoulder in an effort to calculate abduction–adduction at the shoulder joint because significant motion artifact might result from soft-tissue displacement over the scapulohumeral articulation (for a similar problem with the human knee, see Miranda et al., 2013). The amount of wing folding and unfolding was quantified as the span ratio, i.e. the ratio of minimum to maximum wingspan defined as the distance between the sternum and the wrist observed during the upstroke versus the downstroke, respectively (Pennycuick, 1968b; Hubel et al., 2012; von Busse et al., 2012).

Measurements of EMG activity and recruitment intensity
We recorded muscle activity from pectoralis and biceps in four *C. perspicillata* flying at 1–7 m s⁻¹ and in four *E. fuscus* flying at 2–7.9 m s⁻¹. Details about individuals and experiments are provided in Table 1. All conditioning of measurement and extraction of data was performed in Igor Pro v. 6.1 (Wavemetrics). A custom FIR filter was used to remove motion artifact and a semi-automated procedure was then used on the filtered and rectified signals to determine burst onset and offset, which were defined by signal magnitude crossing a minimum activity threshold (two times the standard deviation of the signal magnitude from a given electrode during a period of clear muscle inactivity, typically found during late upstroke). From onset and offset we calculated durations of EMG bursts and duty factors (Figs 1 and 2). After zeroing the baseline, we rectified our EMG recordings and averaged each burst by its duration of activity in the pectoralis and biceps. We then used outlier analyses (Systat v.12) to identify EMG bursts with aberrantly high intensity. All aberrantly high-intensity bursts were excluded from further analysis because the vast majority of these bursts were identified, in the high-speed videos, to be instances of interference between the EMG cable and the bat or the wind tunnel. Absolute EMG burst intensity across electrodes depends upon many factors that can be difficult to control. The remaining EMG burst values were then normalized using the mean intensity for all bursts recorded from a given electrode during a given experiment, resulting in a normalized average burst EMG (aEMG). This method of relating muscle recruitment intensity to flight power is appropriate because the duty factor of activity for both muscles in both species was invariant across
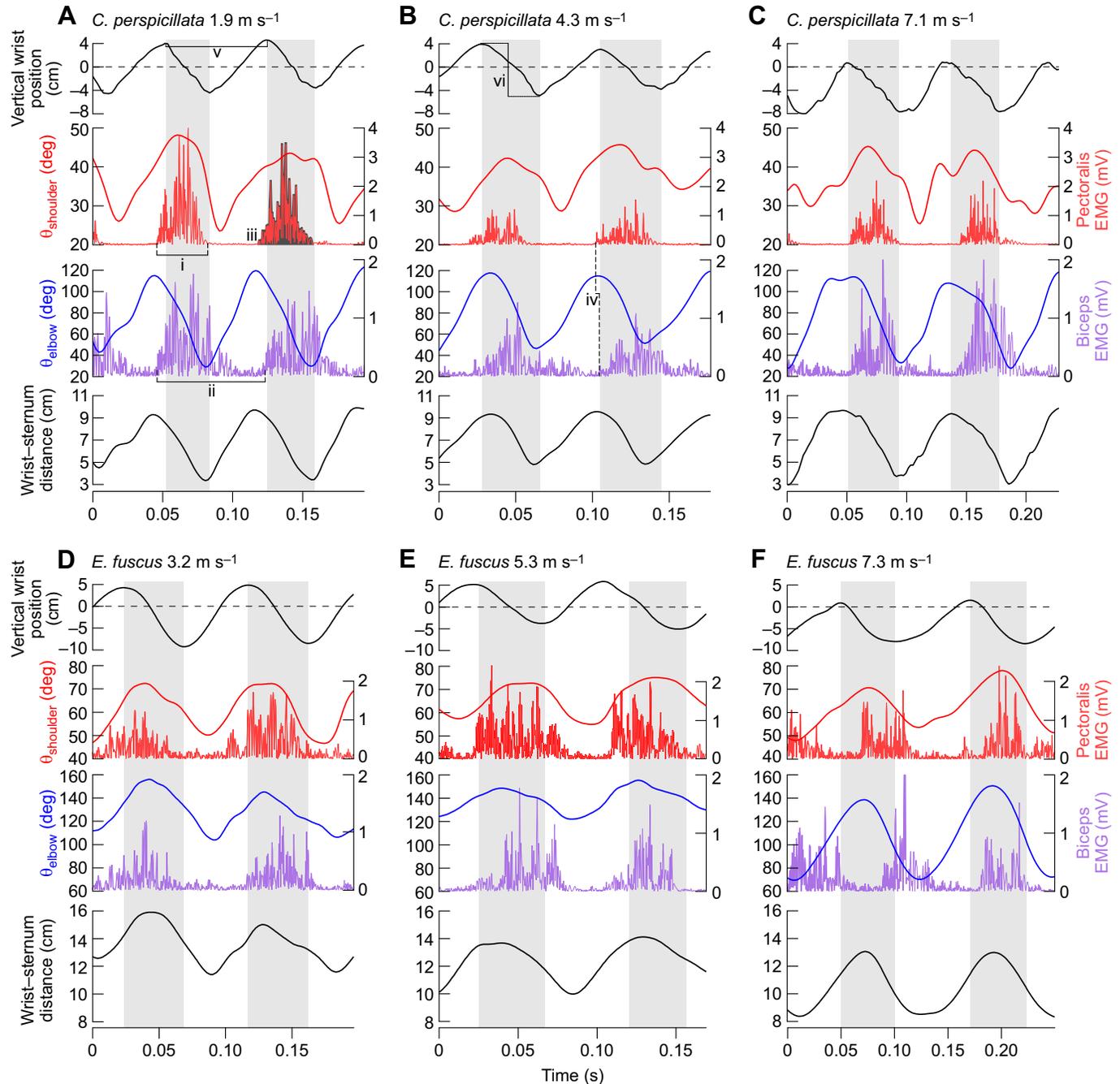
Fig. 1. Sample flight measurements from *Carollia perspicillata* and *Eptesicus fuscus*. Flight measurements at 1.9 m s⁻¹ (A), 4.3 m s⁻¹ (B) and 7.1 m s⁻¹ (C) for *C. perspicillata*, and at 3.2 m s⁻¹ (D), 5.3 m s⁻¹ (E) and 7.3 m s⁻¹ (F) for *E. fuscus*. Top row: vertical wrist position (at zero, the wrist is level with the sternum in the wind tunnel reference coordinate system). Gray bars indicate downstroke. Second row: pectoralis electromyogram (EMG; right *y*-axis) and shoulder angle (angle between humerus and flight direction) (left *y*-axis). Third row: biceps EMG (right *y*-axis) and elbow angle (left *y*-axis). Fourth row: 3D distance from sternum to wrist. Variables measured for each wingbeat (schematically described in A,B) were: (i) EMG burst duration, (ii) EMG cycle duration, (iii) aEMG (average burst intensity, measured as integrated area under the rectified EMG burst, divided by burst duration), (iv) EMG offset, (v) wingbeat duration and (vi) wingbeat amplitude.

flight speeds (Fig. 2I–L). Alternative methods for calculating muscle recruitment intensity, including root mean square and time integral, were explored but did not alter the results and are therefore not reported here.

Analyses

Data exploration, calculation of derived variables and plotting were performed in Systat (v. 12). During exploratory analysis of aEMG

versus flight speed that identified individuals, bouts and flight speeds, we observed a consistent trend of elevated aEMG for the first 3–5 trials in several individuals. We attributed this elevated EMG to transient effects of anesthesia (Sloan, 1998) and therefore, we excluded from analyses all data from the first sequence of flight speeds (3, 4, 5, 6, 7 m s⁻¹) of each individual. To explore the relationships between flight speed and wingbeat cycle duration and amplitude, EMG burst duration and duty factors, we used two-way
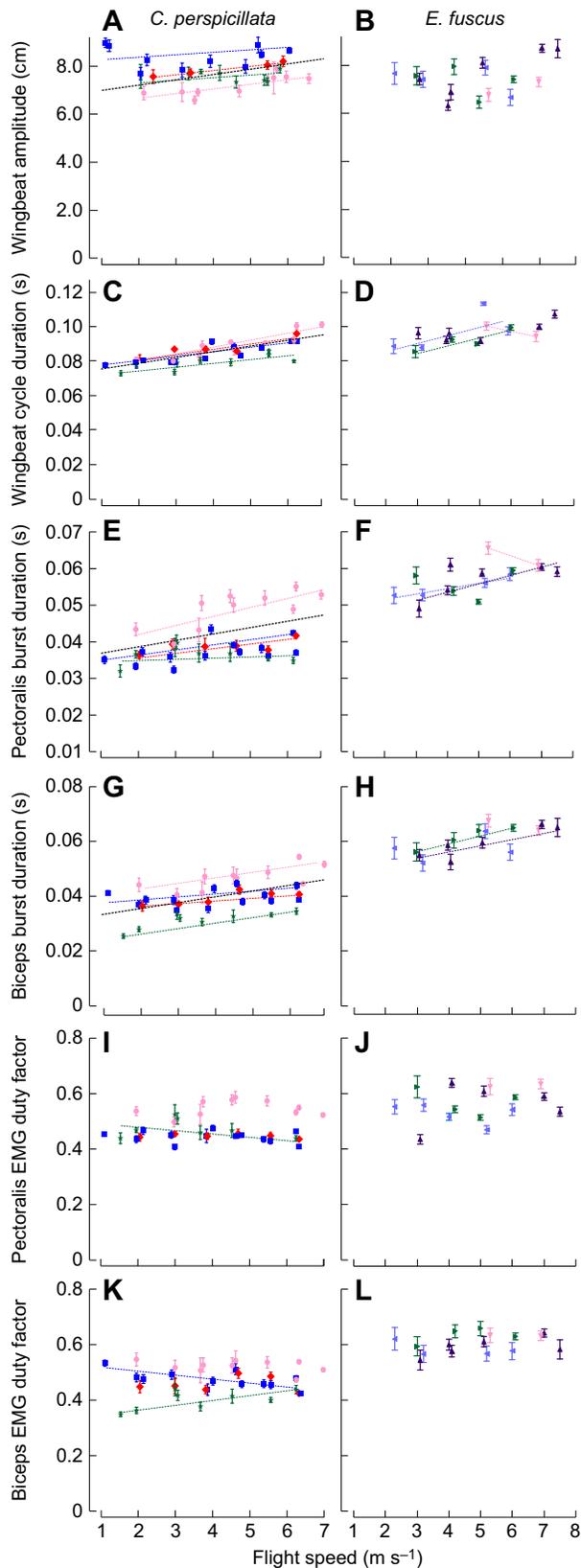
Fig. 2. Wingbeat kinematics and EMG activation patterns in *C. perspicillata* (left column) and *E. fuscus* (right column). Data are means±1 s.d. for 15+ wingbeats at each speed per individual. Each individual is labeled by distinct symbol–color combinations. Data are pooled from repeat experiments on individuals. Black lines are significant global least squares method regression relationships; colored lines are for individuals (*P*<0.05).

ANOVAs (general linear model, implemented in Systat v.12). These tests used the electromyographic or kinematics variable as the dependent factor, flight speed as the independent factor and individual as the random factor. Model simplification was performed where appropriate by removing non-significant individual or interaction terms. We report statistical results for analyses in which data from four bats per species were pooled across one or more experiments at a particular speed. To determine the relationship between dependent variables and flight speed, we analysed at least 15 wingbeats per flight speed for each bat.

When testing hypotheses of speed modulation of pectoralis and biceps aEMG, and particularly considering the prediction of U-shaped modulation patterns, we inspected plots of aEMG versus flight speed for non-linearity. If the plots appeared linear (i.e. lowest aEMG value occurred at the lowest flight speed or aEMG appeared similar across the entire speed range), we used least squares method (LSM) regression (Systat v.11). However, if the lowest aEMG value occurred at an intermediate flight speed ($U_{aEMGmin}$), we used pairwise tests to detect differences between aEMG measurements taken at $U_{aEMGmin}$ versus the highest (U_{max}) and lowest (U_{min}) flight speeds attained by that bat during that experiment. Pairwise tests were also used to determine whether wing folding differed significantly between species at high flight speeds. In all tests, aEMG for pectoralis and biceps were dependent factors, and flight speed was the independent factor. The relationship between biceps aEMG and span ratio across flight speeds was analysed using canonical correlation analyses on individual mean values for each species.

RESULTS

With increases in flight speed, *C. perspicillata* consistently increased wingbeat amplitude, measured as vertical excursion at the wrist, by 5.7% from 7.6±0.82 cm (mean±s.d.) at 2 m s^{-1} to 8.0±0.73 cm at 6 m s^{-1}. ANOVA revealed this increase to be statistically significant (Figs 1 and 2A; $F_{3,263}$=10.53, *P*<0.001; individual effect and interaction term, both *P*<0.0001). Wingbeat cycle duration increased by 20.1%, reaching 0.088±0.008 s at the fastest speeds (Fig. 2C; ANOVA, $F_{2,608}$=240.07, *P*<0.0001; interaction term, *P*<0.0001; individual effect, n.s.). Similarly, burst duration for pectoralis EMG increased by 28.5% to 0.045±0.007 s (Fig. 2E; $F_{2,608}$=194.45, *P*<0.0001; interaction term, *P*<0.0001; individual effect, n.s.), and burst duration for biceps EMG increased by 30.3% to 0.043±0.007 s (Fig. 2G; $F_{2,608}$=235.47, *P*<0.0001; individual effect, *P*<0.0001; interaction term, n.s.). For pectoralis EMG duty factor, LSM regressions showed the significant ANOVA to be driven by a significant relationship for only one bat (Fig. 2I; $F_{2,608}$=75.2, *P*<0.0001; interaction term, *P*<0.0001). As for the pectoralis, the significant effect of speed on biceps EMG duty factor arose from intraspecific variation as biceps EMG duty factor increased in one bat, decreased in another and remained independent of flight speed in the two remaining bats (Fig. 2K; $F_{3,607}$=85.28, *P*<0.0001; individual effect and interaction term, both *P*<0.0001).

In *E. fuscus*, there was no statistically significant change in wingbeat amplitude across flight speeds (Fig. 2B; $F_{3,504}$=13.70, *P*=0.055; individual effect and interaction term, n.s.). Although wingbeat cycle duration varied significantly among speeds, LSM regressions showed this result to be driven by individual variation; cycle duration increased in two bats and decreased in the other two (Fig. 2D; $F_{3,504}$=15.68, *P*<0.05; individual effect and interaction term, *P*<0.001). EMG burst duration was not speed modulated for pectoralis (Fig. 2F; $F_{3,504}$=43.18, *P*=0.781; individual effect,

$P<0.001$), and the ANOVA for speed-dependent change in EMG burst duration for biceps was only significant for two out of the four bats (Fig. 2H; $F_{3,504}=36.79$; $P<0.01$; individual effect and interaction term, $P<0.0001$). No significant modulation of duty factor was seen for pectoralis (Fig. 2J; $F_{3,504}=13.70$, $P=0.055$; individual effect and interaction term, n.s.) nor for biceps (Fig. 2L; $F_{3,504}=9.63$, $P=0.1$; individual effect and interaction term, $P<0.01$).

In *C. perspicillata*, pectoralis and biceps aEMG varied with respect to flight speed in several ways (Fig. 3). Some bats showed a positive linear relationship between aEMG and flight speed in some experiments (LSM regression, $P<0.0001$), some bats had U-shaped relationships in some experiments, and some bats had U-shaped relationships in repeat experiments (LSM pairwise comparisons; U_{min} and U_{max} versus $U_{aEMGmin}$, $P<0.0001$) (Fig. 4). By contrast, we observed no significant variation in aEMG of pectoralis and biceps with respect to flight speed in *E. fuscus* (Fig. 3; all $P>0.1$).

Activation onset for biceps was near simultaneous with that of pectoralis in both species, with an offset in biceps activation of 0.004 ± 0.004 s in *C. perspicillata* ($N=611$ wingbeats) and a more variable temporal relationship of 0.001 ± 0.011 s in *E. fuscus* ($N=508$ wingbeats). Elbow flexion typically began from early to mid-downstroke but in *C. perspicillata* sometimes began in late upstroke. Elbow extension usually began in early to mid-upstroke; occasionally in *E. fuscus*, however, elbow extension began in late downstroke. Sternum–wrist distance, a measure of arm–wing extension, increased in concert with elbow extension and decreased with elbow flexion (Fig. 1). Span ratio, the ratio of minimum to and maximum wingspan, decreased significantly as flight speed increased in *C. perspicillata* ($F_{1,92}=73.21$, $P=0.001$) but remained constant with flight speed in *E. fuscus* ($F_{1,151}=2.46$, $P=0.12$) (Fig. 5). Biceps aEMG and span ratio were correlated in *C. perspicillata* ($r^2=0.52$, correlation coefficient -0.73, $F_{1,16}=18.28$, $P<0.001$) but not in *E. fuscus* ($r^2=0.015$, correlation coefficient -0.124, $F_{1,17}=0.265$, $P>0.5$). Three-dimensional wing joint kinematics revealed flight in *C. perspicillata* displayed a relatively more flexed shoulder and elbow and hence a more folded wing than in *E. fuscus*, where kinematics were modulated in concert in the shoulder, elbow and wrist (Fig. 6). Thus, in *E. fuscus*, total wing folding decreased with flight speed, so that flight involved gradually less folded wings as speed increased, without a significant change in span ratio.

DISCUSSION

Flapping fliers are subject to challenges associated with lift production for weight support at low speed and countering form drag as speed increases. Given these challenges, we expected two bat species with similar adult body mass, wing size and wing shape to show similar patterns of modulation of aEMG of their pectoralis and biceps muscles with respect to flight speed. We also expected similar speed-dependent patterns of change in wing shape in the two species. Instead, we found clear interspecific differences: muscle activation duration and recruitment intensity for both pectoralis and biceps were consistently modulated with flight speed in *C. perspicillata* but invariant in *E. fuscus*. All aspects of wing kinematics that we quantified here were speed modulated in *C. perspicillata*, and the two species used significantly different strategies for changing wing shape across flight speeds.

Interspecific differences in speed modulation of aEMG

We discovered substantial interspecific differences in aEMG modulation across wind tunnel flight speeds comparable with reported flight speed ranges for the two species [*C. perspicillata*, 2.8–6.6 m s^{-1} (Heithaus and Fleming, 1978); *E. fuscus*, 2.0–9.2 m s^{-1} (Hayward and Davis, 1964; Kurta and Baker, 1990; Falk et al., 2014)]. We observed considerable aEMG modulation in *C. perspicillata*, contrasted by a lack of modulation in *E. fuscus*. This finding is consistent with results for avian pectoralis muscles (Tobalske et al., 2010). In zebra finches, which are small, relatively fast-flying birds, the magnitude of pectoralis aEMG variation is only approximately 15–25% over a substantial range of flight speeds, similar to our observation of 11–17% variation in *E. fuscus*. By contrast, hummingbirds, budgerigars and magpies modulate pectoralis recruitment intensity over a much larger range with changes in flight speed, with a range as high as 75% in magpies (Ellerby and Askew, 2007b; Tobalske et al., 2010, 2005), similar to the variation of over 55% that we observed in *C. perspicillata*. Body size-dependence of both recruitment intensity and contractile mechanics of pectoralis have been suggested for birds (Hagiwara et al., 1968; Tobalske and Dial, 2000; Tobalske et al., 2010). However, this idea has been challenged by respirometry studies (Bundle et al., 2007). In our study, the different patterns of recruitment intensity are clearly not related to body size, given the similarity of our two study species.
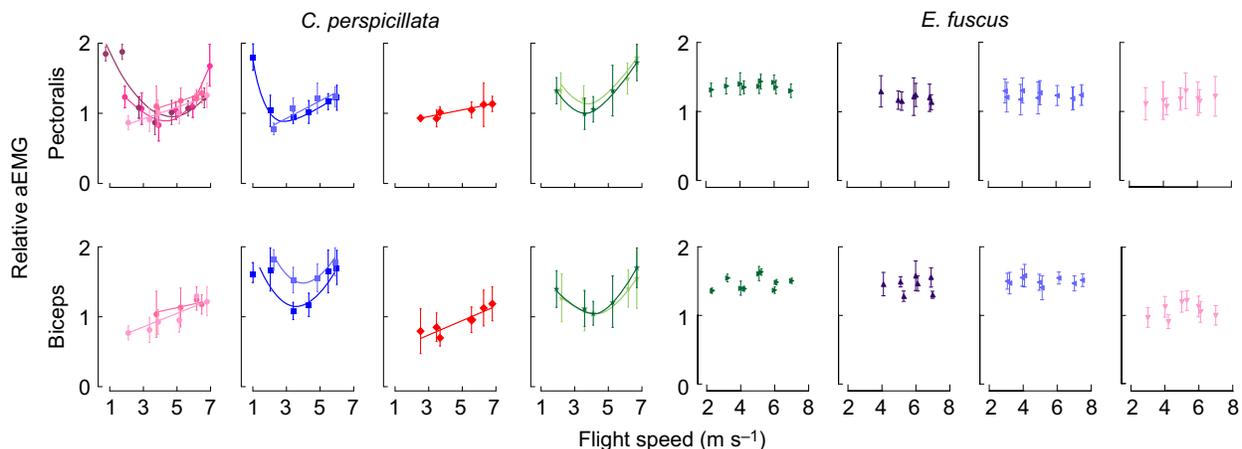

Fig. 3. Relationship between normalized average burst EMG (aEMG) (mean±s.d.) and flight speed in *C. perspicillata* and *E. fuscus*. Top row, pectoralis major; bottom row, biceps brachii short head. Individuals are labeled by distinct symbols, and repeat experiments on an individual are indicated by variations in color tone.
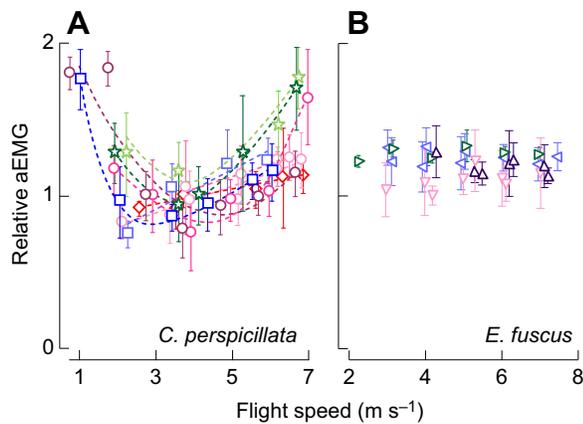
Fig. 4. Pectoralis aEMG versus flight speed. Individuals are labeled by distinct symbols, and repeat experiments on an individual are indicated by variations in color tone. Polynomial fits in A were applied to data for repeat experiments on a given individual. Data are trial means±1 s.d.

The tendency to modulate aEMG with flight speed may, alternatively, be related to the diversity of fiber types present in the musculature. Immunohistochemistry of insectivorous vespertilionid and molossid bats studied to date, including *E. fuscus*, contain a single, fast oxidative-glycolytic and non-fatigueable fiber type (Hermanson, 1997). In contrast, pectoralis in *C. perspicillata* and some closely related phyllostomids (*A. jamaicensis* and *Artibeus lituratus*) contains at least two muscle fiber types (Hermanson, 1997; Hermanson et al., 1998). Both are fast oxidative and non-fatigueable but may be distinctly innervated, and it has been hypothesized that they provide two 'gears' (Hermanson, 1997). It has been proposed that the additional pectoralis fiber type in phyllostomids facilitates hovering and carrying substantial fruit loads prior to consumption, which can increase body mass by as much as 40% (Hermanson, 1997; Hermanson et al., 1998). There is only one fiber type in the pectoralis of finches and hummingbirds, although two fiber types are observed in larger-bodied birds, in which the more glycolytic type is hypothesized to drive take-off wingbeats (Rosser and George, 1986; Dial et al., 1987; Sokoloff et al., 1998; Welch and Altshuler, 2009), which possesses a single myosin heavy-chain isoform (Velten and Welch, 2014). Muscle fibers of smaller avian pectoralis muscles may be capable of a wider range of efficient
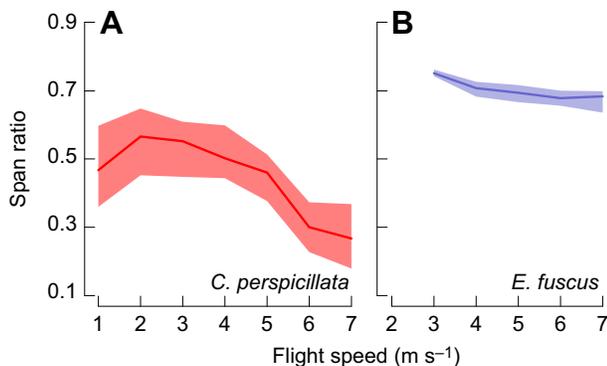

Fig. 6. Maximum joint flexion and extension with respect to flight speed in *C. perspicillata* and *E. fuscus*. Maximum joint flexion (dark, downstroke) and extension (light, upstroke) at the shoulder, elbow and wrist with respect to flight speed in *C. perspicillata* (left column) and *E. fuscus* (right column). Data are median lines with quartile envelopes with repeat experiments on all individuals pooled. The wing is more extended at the shoulder and elbow in *E. fuscus* than in *C. perspicillata* but *E. fuscus* modulates joint flexion–extension with respect to flight speed and therefore wing folding decreases with flight speed in this species.

contractile velocities than is generally expected for vertebrate skeletal muscle (Tobalske et al., 1997). In bats, we observed invariant pectoralis aEMG across flight speeds in *E. fuscus*, which has a single pectoralis muscle fiber type. By contrast, *C. perspicillata*, which has two pectoralis fiber types, modulates pectoralis aEMG with flight speed. Additional muscle fiber diversity in phyllostomids might thus allow for modulation of pectoralis aEMG and power production associated with changes in flight speed.

Flight speed-independence of pectoralis aEMG in *E. fuscus*

The lack of variation in aEMG with flight speed in *E. fuscus* is notable for several reasons. This finding contrasts with the modulation observed in *C. perspicillata*, and it is especially striking given the similarities in body mass and the span, area and aspect ratio of the wings of the two species. The result also contrasts with the majority of studies of bird flight muscles to date (summarized in Tobalske et al., 2010), and is not consistent with the idea that flight power is higher at extreme than intermediate speeds (Pennycuick, 1968a; Rayner, 1979). In this study, we did not, however, record flights below 2 or above 8 m s^{-1}, and more extensive data could change these results; it is possible we did not sample the steeper portions of a pectoralis aEMG versus flight speed curve that is U-shaped but flat over a range of moderate speeds. However, the range of speeds over which we collected measurements, 2.0–8.0 m s^{-1}, is close to the reported natural

Fig. 5. Span ratio in *C. perspicillata* and *E. fuscus*. Span ratio in *C. perspicillata* (A) decreases with speed and is lower in magnitude than the relatively flight speed-invariant span ratio in *E. fuscus* (B). Data are median lines with quartile envelopes of the ratio between minimum and maximum distance between the wrist and sternum (upstroke versus downstroke). See also Fig. 6.
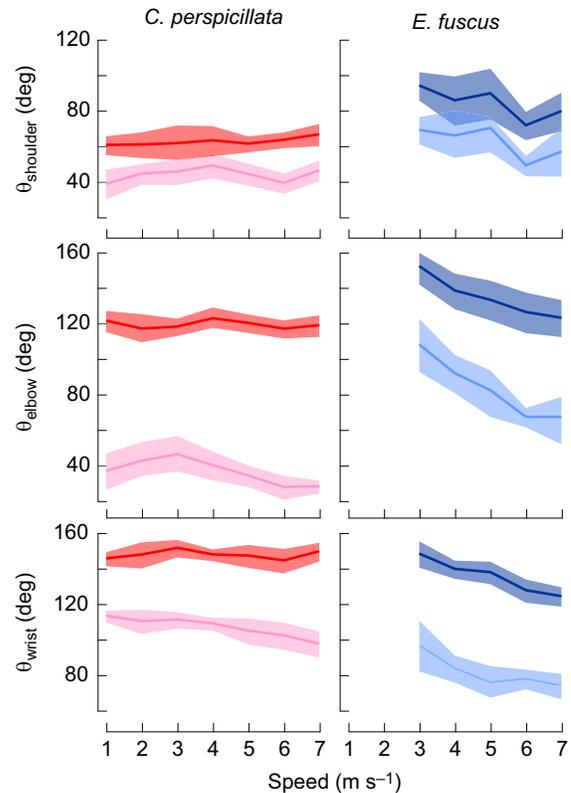
range of over-ground flight speeds for the species, 2.0–9.2 m s^{-1} (Hayward and Davis, 1964; Kurta and Baker, 1990; Falk et al., 2014).

In bats, pectoralis power consumption is likely a smaller component of flight energetics than in birds because a greater number of muscles contribute to aerodynamic force production. These muscles include serratus anterior and subscapularis, which are relatively more massive in bats than in birds, for whom pectoralis is virtually the sole source for downstroke power (Vaughan, 1959; Hermanson and Altenbach, 1981). Vespertilionids such as *E. fuscus* tend to have downstroke muscles that are relatively more gracile than those of phyllostomids including *C. perspicillata* (Strickler, 1978). Although muscle mass is a relatively crude predictor of force production because it does not take account of fiber architecture, fiber type, leverage due to geometry of muscle attachments and effects of series elastic action, available data suggest that that the pectoralis in *E. fuscus* could be force limited. Depending on how muscle shortening speed is modulated with respect to flight speed, which was not measured in this study, mechanical power production could be a factor that limits mechanical performance of the bat flight apparatus.

It is possible that the flight speed-independence of pectoralis recruitment intensity in *E. fuscus* is compensated for by speed-dependent recruitment of other muscles of the 'downstroke group' (Vaughan, 1959; Hermanson and Altenbach, 1981; Altenbach and Hermanson, 1987). If so, net mechanical power production during downstroke may be subject to modulation with flight speed, even if this phenomenon is not observed within the pectoralis *per se*. Alternatively, *E. fuscus* may maintain power output at similar levels across flight speeds, and redirect aerodynamic force through subtle alterations of three-dimensional wing configuration, overcoming increasing drag at higher speeds by modifying the coefficient of drag. Modulation of flight power by kinematic adjustment has been observed in insect flight (e.g. Vance et al., 2014). A deeper understanding of the relationship between mechanical and aerodynamic power, force production and flight speed in bats might emerge from simultaneous measurements of muscle recruitment intensity for the full downstroke group [pectoralis major, serratus anterior, subscapularis, latissimus dorsi, biceps and teres major (Vaughan, 1970; Hermanson and Altenbach, 1983)] combined with an improved understanding of aerodynamic force production, as can be achieved using, for example, particle image velocimetry of the wake (e.g. Muijres et al., 2011; Hubel et al., 2012) and measurement of metabolic power (von Busse et al., 2013).

Variable modulation of aEMG in *C. perspicillata*
In *C. perspicillata*, we observed variation among individuals in the speed-dependent modulation of aEMG for both pectoralis and biceps, as well as within-individual variation in the speed modulation of pectoralis aEMG, with the relationship being U-shaped on two experiment days for two individuals, and variably U-shaped or linearly increasing on different experiment days for two individuals. This kind of result could arise from differences in electrode placement among individuals with respect to heterogeneous distribution of the two different fiber types, as is the case in the study of the triceps surae of cursorial vertebrates (Edström and Kugelberg, 1968; Totland and Kryvi, 1991). However, the pectoralis of *A. jamaicensis*, a closely related species, shows no fiber type compartmentalization that would cause this kind of result (Hermanson and Altenbach, 1985). In addition, we used magnification and landmark orientation to ensure that our implantation of electrodes was as close as possible to identical within each muscle for each individual. Furthermore, the variation in aEMG is similar to that observed in metabolic power

measurements for the same species, in some cases the same individuals, over this range of flight speeds (von Busse et al., 2013). Relatively high levels of individual variation have been observed previously in bat flight kinematics as well; for instance in response to added loads, *Cynopterus brachyotis* (Pteropodidae) modulated wingbeat kinematics in multiple distinct ways, including increased wingbeat frequency, increased camber and increased wing area (Iriarte-Diaz et al., 2012).

As many muscles likely contribute to control and power production in bat flight (Vaughan, 1959; Hermanson and Altenbach, 1981), a weaker relationship is likely between pectoralis activity and flight metabolic power in bats than in birds and insects, where strong relationships between the mechanical behavior of major flight muscles and whole-animal metabolic power have been reported (Wakeling and Ellington, 1997; Josephson et al., 2001; Hedrick et al., 2003; Askew and Ellerby, 2007; Ellerby and Askew, 2007a,b; Morris and Askew, 2010a,b; Morris et al., 2010). However, our aEMG results for *C. perspicillata*, combined with recent data on metabolic power consumption (von Busse et al., 2013), suggest that correspondence between speed-dependent pectoralis aEMG and metabolic power is still strong in bats, as measured from a single population of study animals in the same experimental setting (Fig. 7).

Muscle action, wing folding kinematics and reduction of drag during high-speed flight
Pectoralis and the short head of biceps brachii are activated nearly simultaneously during downstroke in *C. perspicillata* (Fig. 1). Towards the end of this period, the wing begins to fold in preparation for upstroke, and a traditional functional interpretation is that this strategy renders the upstroke aerodynamically inactive (Aldridge, 1986). However, experimental fluid dynamic measurements have demonstrated that upstrokes produce aerodynamic force in most bat species at most flight speeds (Hedenström and Johansson, 2015; Swartz and Konow, 2015). Mathematical modeling suggests that performing the upstroke with a partially folded wing significantly reduces inertial cost by
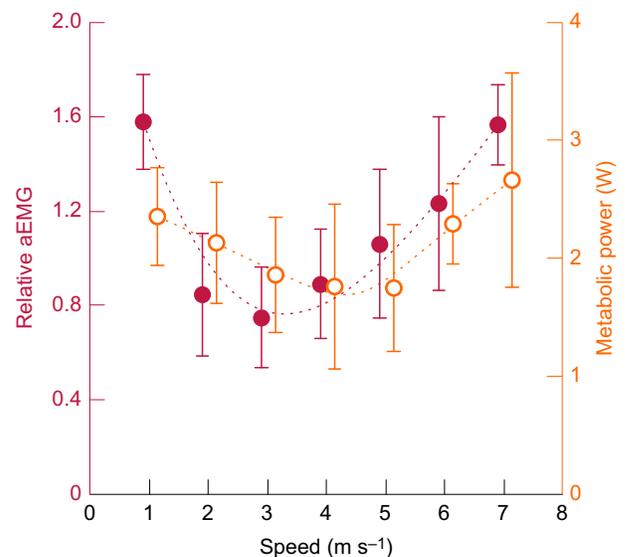

Fig. 7. Comparison of the speed-dependent modulation of pectoralis muscle recruitment and metabolic power consumption for *C. perspicillata*. Closed circles indicate pectoralis muscle recruitment (mean±s.e.m.) whereas open circles indicate metabolic power consumption [from von Busse et al., 2013 (mean±s.e.m.)]. Metabolic and aEMG data for each speed increment have been shifted horizontally for ease of interpretation.

bringing the distal wing elements closer to the wing center of rotation (Riskin et al., 2012). Physical modeling with a bat-like robotic flapper capable of elbow flexion confirms that wing folding significantly reduces the power required to generate lift, but also reduces thrust (Bahlman et al., 2013).

We hypothesized that the two species we studied would use similar strategies for modulating wing flexion–extension with respect to flight speed. Our results ran counter to this expectation and appear related to the observed patterns of muscle recruitment intensity modulation. There was a clear decrease in span ratio with speed in *C. perspicillata* whereas span ratio was relatively invariant and always substantially larger in *E. fuscus*, indicating less relative wing folding during the upstroke than in *C. perspicillata* (Fig. 5). Analyses of specific motions at the shoulder, elbow and wrist (Fig. 6) indicate that in *C. perspicillata* the degree of flexion and extension at each joint show relatively little change over the range of flight speeds studied. However, in *E. fuscus*, peak flexion and peak extension decrease at all joints as speed increase (Fig. 6). Because the observed changes in joint motion occur in concert across flight speeds, span ratio is consistent across speeds in *E. fuscus* (Fig. 5). Therefore, the wing is progressively more folded during upstroke as speed increases in both species; this is reflected in span ratio in *C. perspicillata* but not in *E. fuscus* because span ratio measures only a single linear dimension of wing geometry. 3D kinematics at the level of specific joints reveals a more nuanced picture of wing shape change for the species. In somewhat different ways, the results from both species support the idea that bats reduce form drag with increasing speed, and are consistent with findings from a third bat family, the Molossidae, specifically *Tadarida brasiliensis*, the Brazilian free-tailed bat (Hubel et al., 2012).

The principal action of biceps brachii is elbow flexion and we hypothesized that biceps aEMG and wing folding would be correlated. The significant relationship in *C. perspicillata* showed that biceps aEMG and wing folding increased in concert as flight speed increased. In *E. fuscus*, neither aEMG nor span ratio changed with flight speed, and there is an associated consistency in wing joint flexion–extension. Although bats might use significant elastic energy recoil to power dynamic morphing of their wing configuration (Konow et al., 2015), our results for *E. fuscus* suggest that the amount of mechanical work done by biceps might be constant across flight speeds, in line with our discovery of speed-invariant aEMG for this muscle.

At present, it is not possible to relate the details of bat wing kinematics to aerodynamic force production in a rigorous, mechanistic fashion. However, predictive simulation has recently been employed to gain insight into the effect of wing kinematics on inertial and aerodynamic forces, and resulting flight trajectories and energetics for pigeons (Parslew, 2015). With ongoing work, it will be possible to implement similar models for bat flight.

Conclusions

We observed variation in speed-dependent modulation of recruitment intensity of pectoralis major and biceps brachii in *C. perspicillata*. This variation could be related to the available diversity of muscle fiber types and/or behavioral flexibility inherent to wing form and function in bats. Our finding that pectoralis and biceps recruitment intensity was relatively constant across flight speeds in *E. fuscus* is not predicted by traditional flight power theory, which predicts that more power is required at low and high speeds. The speed independence of pectoralis recruitment intensity in *E. fuscus* suggests that modulating production and delivery of mechanical power in response to demands of changing flight speeds

could involve recruitment of multiple muscles or changes in wing shape in at least some bat species. With the two species in our study, we have only a first glimpse of the comparative biology of motor patterns of the primary flight muscles in Chiroptera. There are many possible explanations for the differences between the two species, and only broader sampling including a greater diversity of taxa can provide the necessary resolution to determine the relative importance among roosting behavior, flight ecology, energetics, evolutionary history and other factors that shape these patterns (Garland and Adolph, 1994). We would benefit from future work that extends our knowledge of muscle activity during flight over a broader range of speeds and activities, beyond these two muscles, and in a more extensive sample of bat diversity.

References
Agnarsson, I., Zambrana-Torrelio, C. M., Flores-Saldana, N. P. and May-Collado, L. J. (2011). A time-calibrated species-level phylogeny of bats (Chiroptera, Mammalia). *PLoS Curr.* **3**, RRN1212.

Aldridge, H. D. J. N. (1986). Kinematics and aerodynamics of the greater horseshoe bat, *Rhinolophus ferrumequinum*, in horizontal flight at various flight speeds. *J. Exp. Biol.* **126**, 479-497.

Altenbach, J. S. and Hermanson, J. W. (1987). Bat flight muscle function and the scapulo-humeral lock. In *Recent Advances in the Study of Bats* (ed. M. B. Fenton, P. Racey and J. V. M. Rayner), pp. 100-118. Cambridge: Cambridge University Press.

Askew, G. N. and Ellerby, D. J. (2007). The mechanical power requirements of avian flight. *Biol. Lett.* **3**, 445-448.

Bahlman, J. W., Swartz, S. M. and Breuer, K. S. (2013). Design and characterization of a multi-articulated robotic bat wing. *Bioinspir. Biomim.* **8**, 016009.

Basmajian, J. and Stecko, G. (1962). A new bipolar electrode for electromyography. *J. Apppl. Physiol.* **17**, 849.

Bergou, A. J., Swartz, S., Breuer, K. Taubin, G. (2011). 3D reconstruction of bat flight kinematics from sparse multiple views. In Computer Vision Workshops (ICCV Workshops), 2011 IEEE International Conference, pp. 1618-1625. IEEE.

Biewener, A. A. (2011). Muscle function in avian flight: achieving power and control. *Philos. Trans. R. Soc. B Biol. Sci.* **366**, 1496-1506.

Biewener, A. A., Farley, C. T., Roberts, T. J. and Temaner, M. (2004). Muscle mechanical advantage of human walking and running: implications for energy cost. *J. Appl. Physiol.* **97**, 2266-2274.

Bundle, M. W., Hansen, K. S. and Dial, K. P. (2007). Does the metabolic rate–flight speed relationship vary among geometrically similar birds of different mass? *J. Exp. Biol.* **210**, 1075-1083.

Cheney, J. A., Konow, N., Middleton, K. M., Breuer, K. S., Roberts, T. J., Giblin, E. L. and Swartz, S. M. (2014). Membrane muscle function in the compliant wings of bats. *Bioinspir. Biomim.* **9**, 025007.

Crook, T. C., Wilson, A. and Hodson-Tole, E. (2010). The effect of treadmill speed and gradient on equine hindlimb muscle activity. *Equine Vet. J.* **42**, 412-416.

Dial, K. P., Kaplan, S. R., Goslow, G. E. and Jenkins, F. A. (1987). Structure and neural control of the pectoralis in pigeons – implications for flight mechanics. *Anat. Rec.* **218**, 284-287.

Dial, K. P., Kaplan, S. R., Goslow, G. E. and Jenkins, F. A. (1988). A functional analysis of the primary upstroke and downstroke muscles in the domestic pigeon (*Columba livia*) during flight. *J. Exp. Biol.* **134**, 1-16.

Edström, L. and Kugelberg, E. (1968). Histochemical composition, distribution of fibres and fatiguability of single motor units. Anterior tibial muscle of the rat. *J. Neurol. Neurosurg. Psychiatry* **31**, 424-433.

Ellerby, D. J. and Askew, G. N. (2007a). Modulation of flight muscle power output in budgerigars *Melopsittacus undulatus* and zebra finches *Taeniopygia guttata*: *in vitro* muscle performance. *J. Exp. Biol.* **210**, 3780-3788.

Ellerby, D. J. and Askew, G. N. (2007b). Modulation of pectoralis muscle function in budgerigars *Melopsitaccus undulatus* and zebra finches *Taeniopygia guttata* in response to changing flight speed. *J. Exp. Biol.* **210**, 3789-3797.

Falk, B., Jakobsen, L., Surlykke, A. and Moss, C. F. (2014). Bats coordinate sonar and flight behavior as they forage in open and cluttered environments. *J. Exp. Biol.* **217**, 4356-4364.

Foehring, R. C. and Hermanson, J. W. (1984). Morphology and histochemistry of flight muscles in free-tailed bats, *Tadarida brasiliensis*. *J. Mammal.* **65**, 388-394.

Garland, T. J. and Adolph, S. C. (1994). Why not to do two-species comparative studies: limitations on inferring adaptation. *Physiol. Zool.* **67**, 797-828.

Gillis, G. B. and Biewener, A. A. (2001). Hindlimb muscle function in relation to speed and gait: *in vivo* patterns of strain and activation in a hip and knee extensor of the rat (*Rattus norvegicus*). *J. Exp. Biol.* **204**, 2717-2731.

Gillis, G. B., Flynn, J. P., McGuigan, P. and Biewener, A. A. (2005). Patterns of strain and activation in the thigh muscles of goats across gaits during level locomotion. *J. Exp. Biol.* **208**, 4599-4611.

Hagiwara, S., Chichibu, S. and Simpson, N. (1968). Neuromuscular mechanisms of wing beat in hummingbirds. *Zeitschrift für vergleichende Physiologie* **60**, 209-218.

Hayward, B. and Davis, R. (1964). Flight speed in western bats. *J. Mammal.* **45**, 236-242.

Hedenström, A. and Johansson, L. C. (2015). Bat flight: aerodynamics, kinematics and flight morphology. *J. Exp. Biol.* **218**, 653-663.

Hedrick, T. L. and Biewener, A. A. (2007). Low speed maneuvering flight of the rose-breasted cockatoo (*Eolophus roseicapillus*). I. Kinematic and neuromuscular control of turning. *J. Exp. Biol.* **210**, 1897-1911.

Hedrick, T. L., Tobalske, B. W. and Biewener, A. A. (2003). How cockatiels (*Nymphicus hollandicus*) modulate pectoralis power output across flight speeds. *J. Exp. Biol.* **206**, 1363-1378.

Heithaus, E. R. and Fleming, T. H. (1978). Foraging movements of a frugivorous bat, *Carollia perspicillata* (Phyllostomatidae). *Ecol. Monogr.* **48**, 127-143.

Hermanson, J. W. (1997). Chiropteran muscle biology: a perspective from molecules to function. In *Bats: Phylogeny, Morphology, Echolocation, and Conservation Biology* (ed. T. H. Kunz and P. A. Racey), pp. 127-139. Washington, D. C: Smithsonian Institution Press.

Hermanson, J. W. and Altenbach, J. S. (1981). Functional anatomy of the primary downstroke muscles in the pallid bat, *Antrozous pallidus*. *J. Mamm.* **62**, 795-800.

Hermanson, J. W. and Altenbach, J. S. (1983). The functional anatomy of the shoulder of the Pallid Bat, *Antrozous pallidus*. *J. Mammal.* **64**, 62-75.

Hermanson, J. W. and Altenbach, J. S. (1985). Functional anatomy of the shoulder and arm of the fruit-eating bat *Artibeus jamaicensis*. *J. Zool.* **205**, 157-177.

Hermanson, J. W., Ryan, J. H., Cobb, M. A., Bentley, J. and Schutt, W. A.Jr (1998). Histochemical and electrophoretic analysis of the primary flight muscle of several phyllostomid bats. *Can. J. Zool.* **76**, 1983-1992.

Hoyt, D. F., Wickler, S. J., Biewener, A. A., Cogger, E. A. and De La Paz, K. L. (2005). *In vivo* muscle function vs speed. I. Muscle strain in relation to length change of the muscle-tendon unit. *J. Exp. Biol.* **208**, 1175-1190.

Hubel, T. Y., Hristov, N. I., Swartz, S. M. and Breuer, K. S. (2012). Changes in kinematics and aerodynamics over a range of speeds in *Tadarida brasiliensis*, the Brazilian free-tailed bat. *J. R. Soc. Interface* **9**, 1120-1130.

Hubel, T. Y., Hristov, N. I., Swartz, S. M. and Breuer, K. S. (2016). Wake structure and kinematics in two insectivorous bats. *Philos. Trans. R. Soc. B Biol. Sci.* **371**.

Iriarte-Diaz, J., Riskin, D. K., Breuer, K. S. and Swartz, S. M. (2012). Kinematic plasticity during flight in fruit bats: Individual variability in response to loading. *PLoS ONE* **7**, e36665.

Josephson, R. K., Malamud, J. G. and Stokes, D. R. (2001). The efficiency of an asynchronous flight muscle from a beetle. *J. Exp. Biol.* **204**, 4125-4139.

Konow, N., Cheney, J. A., Roberts, T. J., Waldman, J. R. S. and Swartz, S. M. (2015). Spring or string: does tendon elastic action influence wing muscle mechanics in bat flight? *Proc. R. Soc. B Biol. Sci.* **282**.

Koteja, P., Swallow, J. G., Carter, P. A. and Garland, T.Jr (1999). Energy cost of wheel running in house mice: implications for coadaptation of locomotion and energy budgets. *Physiol. Biochem. Zool.* **72**, 238-249.

Kurta, A. and Baker, R. H. (1990). *Eptesicus fuscus. Mammalian Species Accounts.* **356**, 1-10.

Marsh, R. L., Ellerby, D. J., Carr, J. A., Henry, H. T. and Buchanan, C. I. (2004). Partitioning the energetics of walking and running: swinging the limbs is expensive. *Science* **303**, 80-83.

Miranda, D. L., Rainbow, M. J., Crisco, J. J. and Fleming, B. C. (2013). Kinematic differences between optical motion capture and biplanar videoradiography during a jump–cut maneuver. *J. Biomech.* **46**, 567-573.

Morris, C. R. and Askew, G. N. (2010a). Comparison between mechanical power requirements of flight estimated using an aerodynamic model and *in vitro* muscle performance in the cockatiel (*Nymphicus hollandicus*). *J. Exp. Biol.* **213**, 2781-2787.

Morris, C. R. and Askew, G. N. (2010b). The mechanical power output of the pectoralis muscle of cockatiel (*Nymphicus hollandicus*): the *in vivo* muscle length trajectory and activity patterns and their implications for power modulation. *J. Exp. Biol.* **213**, 2770-2780.

Morris, C. R., Nelson, F. E. and Askew, G. N. (2010). The metabolic power requirements of flight and estimations of flight muscle efficiency in the cockatiel (*Nymphicus hollandicus*). *J. Exp. Biol.* **213**, 2788-2796.

Muijres, F. T., Johansson, L. C., Winter, Y. and Hedenström, A. (2011). Comparative aerodynamic performance of flapping flight in two bat species using time-resolved wake visualization. *J. R. Soc. Interface* **8**, 1418-1428.

Norberg, U. M. and Rayner, J. M. V. (1987). Ecological morphology and flight in bats (Mammalia, Chiroptera) - wing adaptations, flight performance, foraging strategy and echolocation. *Philos. Trans. R. Soc. Lond. B Biol. Sci.* **316**, 337-427.

Parslew, B. (2015). Predicting power-optimal kinematics of avian wings. *J. R. Soc. Interface* **12**, 20140953.

Pennycuick, C. J. (1968a). Power requirements for horizontal flight in the pigeon *Columba livia*. *J. Exp. Biol.* **49**, 527-555.

Pennycuick, C. J. (1968b). A wind-tunnel study of gliding flight in the pigeon *Columba livia*. *J. Exp. Biol.* **49**, 509-526.

Rayner, J. M. V. (1979). A new approach to animal flight mechanics. *J. Exp. Biol.* **80**, 17-54.

Riskin, D. K., Bergou, A., Breuer, K. S. and Swartz, S. M. (2012). Upstroke wing flexion and the inertial cost of bat flight. *Proc. R. Soc. B* **279**, 2945-2950.

Roberts, T., Kram, R., Weyand, P. and Taylor, C. (1998). Energetics of bipedal running. I. Metabolic cost of generating force. *J. Exp. Biol.* **201**, 2745-2751.

Robertson, A. M. B. and Biewener, A. A. (2012). Muscle function during takeoff and landing flight in the pigeon (*Columba livia*). *J. Exp. Biol.* **215**, 4104-4114.

Rosser, B. W. C. and George, J. C. (1986). The avian pectoralis: histochemical characterization and distribution of muscle fiber types. *Can. J. Zool.* **64**, 1174-1185.

Schunk, C. Swartz, S. M. and Breuer, K. S. (2017). The influence of aspect ratio and stroke pattern on force generation of a bat-inspired membrane wing. *Interface Focus* **7**, 20160083.

Shi, J. J. and Rabosky, D. L. (2015). Speciation dynamics during the global radiation of extant bats. *Evolution* **69**, 1528-1545.

Sloan, T. B. (1998). Anesthetic effects on electrophysiologic recordings. *J. Clin. Neurophys.* **15**, 217-226.

Sokoloff, A. J., Ryan, J. M., Valerie, E., Wilson, D. S. and Goslow, G. E. (1998). Neuromuscular organization of avian flight muscle: Morphology and contractile properties of motor units in the pectoralis (pars thoracicus) of pigeon (*Columba livia*). *J. Morphol.* **236**, 179-208.

Strickler, T. L. (1978). *Functional Osteology and Myology of the Shoulder in Chiroptera*. Basel: Karger.

Swartz, S. M. and Konow, N. (2015). Advances in the study of bat flight: the wing and the wind. *Can. J. Zool.* **93**, 977-990.

Tobalske, B. W. and Dial, K. P. (2000). Effects of body size on take-off flight performance in the Phasianidae (Aves). *J. Exp. Biol.* **203**, 3319-3332.

Tobalske, B. W., Olson, N. E. and Dial, K. P. (1997). Flight style of the black-billed magpie: variation in wing kinematics, neuromuscular control, and muscle composition. *J. Exp. Zool.* **279**, 313-329.

Tobalske, B. W., Puccinelli, L. A. and Sheridan, D. C. (2005). Contractile activity of the pectoralis in the zebra finch according to mode and velocity of flap-bounding flight. *J. Exp. Biol.* **208**, 2895-2901.

Tobalske, B. W., Biewener, A. A., Warrick, D. R., Hedrick, T. L. and Powers, D. R. (2010). Effects of flight speed upon muscle activity in hummingbirds. *J. Exp. Biol.* **213**, 2515-2523.

Totland, G. K. and Kryvi, H. (1991). Distribution patterns of muscle fibre types in major muscles of the bull (*Bos taurus*). *Anat. Embryol.* **184**, 441-450.

Vance, J. T., Altshuler, D. L., Dickson, W. B., Dickinson, M. H. and Roberts, S. P. (2014). Hovering flight in the honeybee *Apis mellifera*: kinematic mechanisms for varying aerodynamic forces. *Physiol. Biochem. Zool.* **87**, 870-881.

Vaughan, T. A. (1959). Functional morphology of three bats: *Eumops, Myotis, Macrotus. Univ. Kansas Publ., Mus. Nat. Hist.* **12**, 1-153.

Vaughan, T. A. (1970). The muscular system. In *The Biology of Bats*, Vol. 1 (ed. W. A. Wimsatt), pp. 140-194. New York: Academic Press.

Velten, B. P. and Welch, K. C. (2014). Myosin heavy-chain isoforms in the flight and leg muscles of hummingbirds and zebra finches. *Am. J. Physiol. Regul. Integr. Comp. Physiol.* **11**, 845-851.

von Busse, R., Hedenström, A., Winter, Y. and Johansson, L. C. (2012). Kinematics and wing shape across flight speed in the bat, *Leptonycteris yerbabuenae*. *Biol. Open* **1**, 1226-1238.

von Busse, R., Swartz, S. M. and Voigt, C. C. (2013). Flight metabolism in relation to speed in Chiroptera: testing the U-shape paradigm in the short-tailed fruit bat *Carollia perspicillata*. *J. Exp. Biol.* **216**, 2073-2080.

Wakeling, J. and Ellington, C. (1997). Dragonfly flight. III. Lift and power requirements. *J. Exp. Biol.* **200**, 583-600.

Weibel, E. R., Taylor, C. R. and Bolis, L. (1998). *Principles of Animal Design: the Optimization and Symmorphosis Debate*. Cambridge: Cambridge University Press.

Welch, K. C., Jr and Altshuler, D. L. (2009). Fiber type homogeneity of the flight musculature in small birds. *Comp. Biochem. Physiol. B Biochem. Mol. Biol.* **152**, 324-331.

Wolf, M., Johansson, L. C., von Busse, R., Winter, Y. and Hedenström, A. (2010). Kinematics of flight and the relationship to the vortex wake of a Pallas' long tongued bat (*Glossophaga soricina*). *J. Exp. Biol.* **213**, 2142-2153.